Tribology Letters (2024) 72:101
https://doi.org/10.1007/s11249-024-01898-6

ORIGINAL PAPER

Ionic Liquids as Extreme Pressure Additives for Bearing Steel Applications

Mariana T. Donato[1,2,3] · Pranjal Nautiyal[3] · Jonas Deuermeier[4] · Luís C. Branco[2] · Benilde Saramago[1] · Rogério Colaço[5] · Robert W. Carpick[3]

Received: 6 February 2024 / Accepted: 24 July 2024 / Published online: 2 August 2024

Abstract

The protection of steel surfaces from wear under extreme pressure conditions is of major importance in several industries as it provides better performance and longer life of machinery. The motivation for this work was to study the lubrication of steel by ionic liquids (ILs), which have recently emerged as greener alternatives to commercial lubricants and additives. Three ILs based on sulfur-containing anions, used as 2-wt% additives in polyethylene glycol base oil (MW 200; PEG 200), were tested in the lubrication of ASTM 52100 bearing steel contacts in extreme pressure conditions (under mixed lubrication with a Hertzian pressure of 1.12 GPa) using a mini traction machine (MTM). Due to the poor resistance to corrosion of bearing steel, a semi-ester of succinic acid derivative corrosion inhibitor (Lanxess RC 4801) was added to the mixtures at a 1 wt% concentration. The ILs 1-hexyl-methylimidazolium trifluoromethanesulfonate ([C_6mim][TfO]) and 1-hexyl-4-picolinium trifluoromethanesulfonate ([C_6-4-pic][TfO]) revealed promising results in terms of surface protection of bearing steel. In contrast, 4-picolinium hydrogen sulfate ([4-picH][HSO_4]) as 2-wt% additive to PEG 200 + 1% RC 4801 did not show any improvement in wear performance compared to neat PEG 200 + 1% RC 4801. PEG 200 + 2% [C_6mim][TfO] + 1%RC 4801 allowed for a decrease in wear up to ~ 76% and PEG 200 + 2% [C_6-4-pic][TfO] + 1%RC 4801 up to ~ 46% when compared with neat PEG 200 + 1% RC 4801. Optical microscopy images suggest the formation of an adsorbed layer, which was further supported by chemical analysis via x-ray photoelectron spectroscopy (XPS) data for [C_6mim][TfO].

Graphical abstract

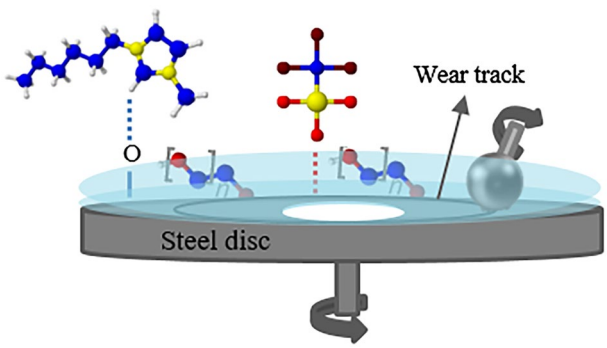

Keywords Friction · Ionic liquids · Lubricant additives · Steel · Wear

Extended author information available on the last page of the article

1 Introduction

Steel is widely used in bearings of vehicle parts, turbines, engines, and varied manufacturing equipment as it is a hard and resistant material [1]. Direct steel-on-steel contact that occurs due to a lack of efficient lubrication or harsh conditions leads to energy losses and increased material damage or failure, which represents a substantial challenge for several industries [2, 3]. Commercial lubricants are usually composed of several additives designed for protecting the contacting surfaces from wear. Ionic liquids (ILs) have emerged as potential anti-wear lubricants and/or additives to counteract wear under harsh conditions. ILs are organic salts with melting points below 100 °C, composed by cation/anion combinations that can be tuned according to the desired final application. They have several appealing properties, such as high chemical and thermal stability, almost negligible vapor pressure (thus helping render them as environmentally friendly compounds), non-flammability, ease in dissolving organic, inorganic, and polymeric materials, and high ionic conductivity [4]. In addition, being highly polar compounds, in contrast to most additives used in synthetic or mineral oils that are non-polar, ILs are highly surface active, presenting a strong tendency to adsorb on metal surfaces [5]. One drawback of ILs is their high cost, which is why they have recently been used as additives at low concentrations in commonly used base oils instead of as base oils themselves [6–9].

ILs in general and protic ILs (PILs) in particular have been shown to exhibit substantial benefits as lubricant additives for several types of contacting materials, including steel [9–13]. For example, Khatri et al. [14] studied fatty acid-derived trioctylphosphonium cation-based PILs with various alkyl chain lengths as additives to polyethylene glycol 200 (PEG 200). The addition of PILs led to a reduction in friction between 28 and 41%, as well as a wear decrease of 15–32% in the mixed/boundary lubrication regime when compared to neat base oil. The improvement in tribological properties was attributed to phosphorous-containing tribofilms formed on the steel surfaces. Horng et al. [15] reported tert-octylamine oleate and diethanolamine oleate PILs as additives to water, showing improved tribological performance: friction was reduced up to 80% and wear up to 85% when compared to water. This was attributed to the formation of an adsorption layer on the surfaces composed of iron oxides. Iglesias et al. [16] studied three PILs—2-hydroxyethylammonium 2-ethylhexanoate, 2-hydroxymethylammonium 2-ethylhexanoate, and 2-hydroxydimethyl-ammonium 2-ethylhexanoate—as neat lubricants and as additives to a mineral oil. All PILs showed reduced friction and wear up to 19.5% and 48%, respectively. The same group also studied ammonium-based PILs as 1-wt.% additives to a mineral oil at room temperature and 100 °C.[17] Friction was reduced after adding the PILs at each temperature by 29% and 35.5%, respectively, attributed to increased levels of oxygen and carbon in the tribolayer formed in the wear track. More recently, Hu et al.[18] studied the lubricating performance of two trialkylammonium carboxylate PILs with different alkyl chain size, as additives to polyalphaolefin (PAO) at room temperature and low temperatures. At room temperature, the shorter alkyl chain PIL showed the best performance, while at low temperature (− 20 °C) both PILs revealed excellent wear reduction due to the formation of ordered adsorbed films, although their friction reduction was not evident.

The behavior of ILs in mixed/boundary lubrication conditions has been discussed in several papers, with the aim of understanding how these compounds could react with the surfaces and protect them from friction and wear. Recently, Mangolini et al. [19] reviewed the advances in nanotribology of ILs, describing the lubrication mechanisms of ILs by the formation of adsorbed and confined layers between two solid surfaces. However, several questions regarding the tribological behavior of ILs remain unanswered. For example, the effect of temperature is not widely reported and properties of ILs' layers should be more deeply studied.

With the aim of studying the performance of lubricant additives under mixed sliding/rolling conditions representative of gears and bearings, three ILs, which demonstrated very good lubrication capacity for stainless steel/silicon and silicon/silicon contacts in previous studies [7, 8, 20], were chosen to be tested as lubricants for ASTM 52100 bearing steel. The chosen ILs were 1-hexyl-methylimidazolium trifluoromethanesulfonate ([C_6mim][TfO]), 1-hexyl-4-picolinium trifluoromethanesulfonate ([C_6-4-pic][TfO]), and 4-picolinium hydrogen sulfate ([4-picH][HSO_4]), used as 2 wt% additives in base oil PEG 200.

The structures of the studied liquids are shown in Fig. 1. The corrosive behavior of the liquids was considered since ASTM 52100 steel with its low chromium level has poor resistance to corrosion [21]. Preliminary tests confirmed

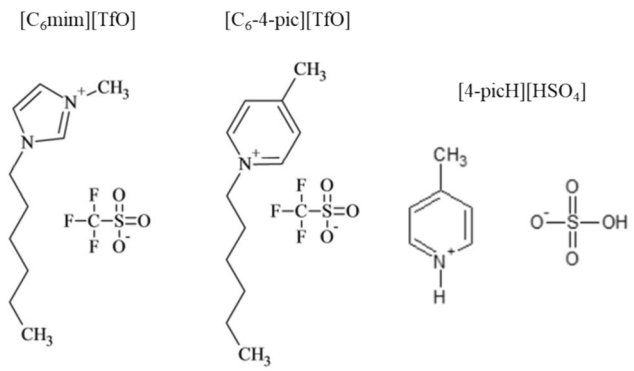

Fig. 1 Chemical structures of the studied ionic liquids

that addition of corrosion inhibitors was required and so a semi-ester of succinic acid derivative corrosion inhibitor (Lanxess RC 4801) was used (see Experimental Section for more details).

The tribological properties were assessed, namely traction and wear, and the worn surfaces of both balls and disks were imaged optically and when possible, analyzed chemically to gain insight on wear mechanisms.

2 Results and Discussion

2.1 Corrosion Experiments

ILs can sometimes be corrosive of steel [22, 23]—especially if their water content is high—and indeed corrosion of the 52,100 steel surfaces used here was observed for all of our fluids. A corrosion inhibitor, RC 4801, a succinic acid semi-ester derivative (acid value: 160 mg KOH/g), was added to the ionic systems at 1 wt% concentration, and the corrosion inhibition capability was evaluated. Although PEG 200 + 2% [C_6mim][TfO] and PEG 200 + 2% [C_6-4-pic][TfO], the two less chemically aggressive formulations, both corroded the steel when no corrosion inhibitor was used, adding 1 wt% of corrosion inhibitor was sufficient to prevent corrosion. Optical microscopy images of the steel surfaces after contacting the two tested ILs with and without corrosion inhibitor are presented in Figure S1 in the Supporting Information.

In contrast, the addition of 1% of corrosion inhibitor did not prevent corrosion in the case of PEG200 + 2%[4-picH][HSO_4], even when a higher concentration (5 wt.%) of the corrosion inhibitor was used. Optical microscopy images showing signs of corrosion for this IL are presented in Figure S2 in the Supporting Information. Considering these results, additional tests were carried out only with PEG 200 + 2% [C_6mim][TfO] + 1%RC 4801 and PEG 200 + 2% [C_6-4-pic][TfO] + 1%RC 4801.

2.2 Traction Coefficient Measurements

The viscosities of PEG 200 + 1% RC 4801, PEG200 + 2% [C_6-4-pic][TfO] + 1% RC 4801, and PEG200 + 2% [C_6mim][TfO] + 1% RC 4801 were measured as a function of temperature from 25 to 60 °C, prior to the tribological tests. The results are presented in Figure S3 (Supporting Information), which shows that the three mixtures have similar, low viscosities over the entire temperature range.

Stribeck curves (traction coefficient *vs*. entrainment speed) obtained for the mixtures of ILs + PEG 200 at 60 ° from 2000 to 7 mm·s^{-1} entrainment speed are shown in Fig. 2. The measurements were performed under mixed sliding/rolling contact conditions through the application

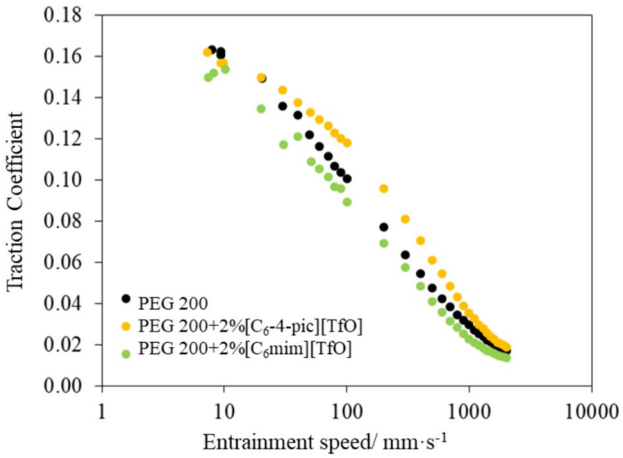

Fig. 2 Stribeck curves obtained at 50 N and 60 °C with 50% SRR, from 2000 to 7 mm·s^{-1} entrainment speed, for PEG 200 + 1% RC 4801, PEG 200 + 2% [C_6-4-pic][TfO] + 1% RC 4801, and PEG 200 + 2% [C_6mim][TfO] + 1% RC 4801. These results were obtained at least in duplicate

of a slide-to-roll ratio (SRR) of 50%, which is given by the following equation:

$$\mathrm{SRR} = \frac{u_D - u_B}{U}, \tag{1}$$

where u_B is the ball speed, u_D is the disk speed, and U is the entrainment speed, defined as $(u_B + u_D)/2$.

Although the differences in the Stribeck curves are small, at low and intermediate speeds, the mixture with [C_6mim][TfO] exhibited a slight decrease in traction relative to the value obtained without the IL (neat PEG), while [C_6-4-pic][TfO] exhibited a slight increase in the traction. The minimum film thickness, h_0, was calculated according to elastohydrodynamic lubrication (EHL) theory using the Hamrock–Dowson model [24] for an entrainment speed of 10 mm·s^{-1}. The obtained value, 2.25 nm, when compared with the composite surface roughness yields a specific film thickness λ of 0.45, indicating mixed lubricating conditions ($0.06 < \lambda < 0.6$) [25]. Calculation details are at the end of the Supporting Information. It is interesting to note that, at high speed, the traction coefficient becomes independent of the additive composition and has similar values for the three liquids. Since in EHL the film thickness increases significantly with speed ($h_0 \propto U^{0.68}$), this indicates that the traction differences seen at lower speeds should be attributed to adsorption of the IL's on the steel surfaces.

In order to assess wear performance of the ILs under aggressive mixed lubricating conditions, subsequent tests were performed at the speed of 10 mm·s^{-1} under the same conditions (50 N, 1.12 GPa Hertz contact pressure, 60 °C, $\lambda = 0.45$).

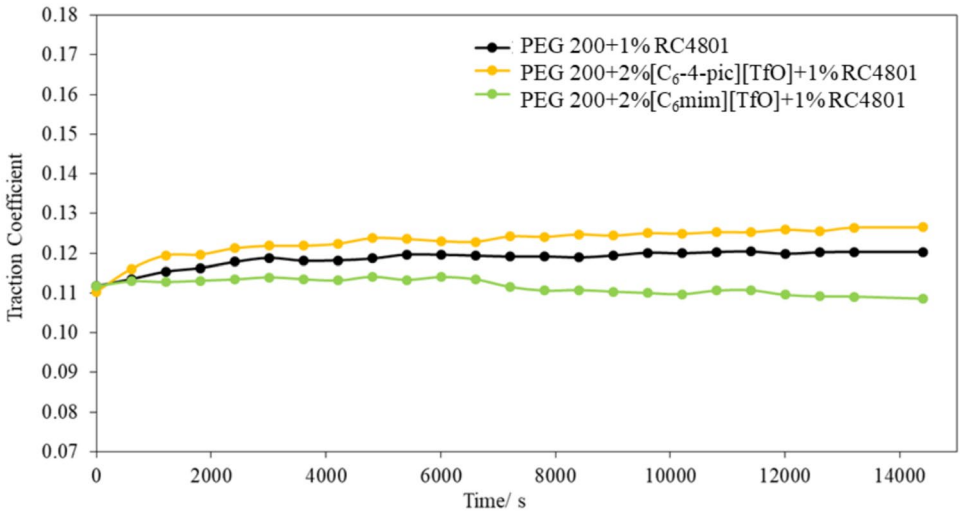

Fig. 3 Traction coefficient *vs*. time for 52,100 steel/steel tribopairs at an entrainment speed of 10 mm·s^{-1} and under the load of 50 N for the studied liquids (1.12 GPa Hertz contact pressure, 50% SRR, 60 °C, $\lambda = 0.45$)

Traction measurements were obtained in four hour tests in the mixed lubrication regime, each with new, washed 52,100 ball/disk pairs as described in the Methods section. The results are presented in Fig. 3, where a slight improvement (up to 12%) of the traction coefficient for PEG 200 + 2% [C_6mim][TfO] + 1%RC 4801 when compared to neat PEG 200 + 1%RC 4801 is seen, consistent with the Stribeck curves in Fig. 2.

2.3 Surface Characterization

After the MTM experiments, all of the ball and disk surfaces were imaged by white light interferometry (WLI) and the wear profiles were obtained. From this, the wear volumes were obtained for the balls and disks and are shown in Fig. 4. These values were calculated based on the mean of at least four cross-sectional profiles for each sample.

For the steel balls, PEG 200 + 2% [C_6-4-pic][TfO] + 1%RC 4801 led to a reduction in the volume to ~ 46% of the value for neat PEG 200 + 1%RC 4801, while the reduction for PEG 200 + 2% [C_6mim][TfO] + 1%RC 4801 was ~ 76%. For the disks, the addition of [C_6-4-pic][TfO] reduced the wear volume to ~ 89% of the value for neat PEG 200 + 1%RC 4801, while [C_6mim][TfO] reduced the wear volume to ~ 65%. Thus, [C_6mim][TfO] showed the best tribological performance overall, with lower traction coefficient, as well as lower ball and disk wear.

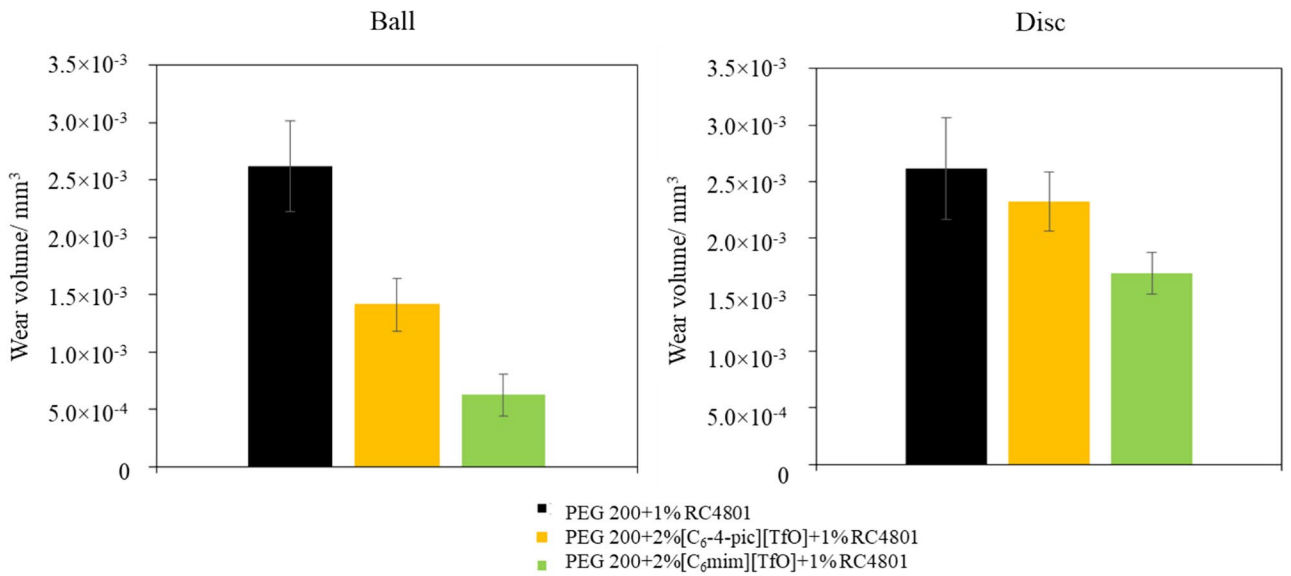

Fig. 4 Average wear volumes obtained for steel balls (left image) and disks (right image) after long tribological tests (4 h) at an entrainment speed of 10 mm·s^{-1} and under the load of 50 N. The errors are ± standard deviation ($n \geq 4$)

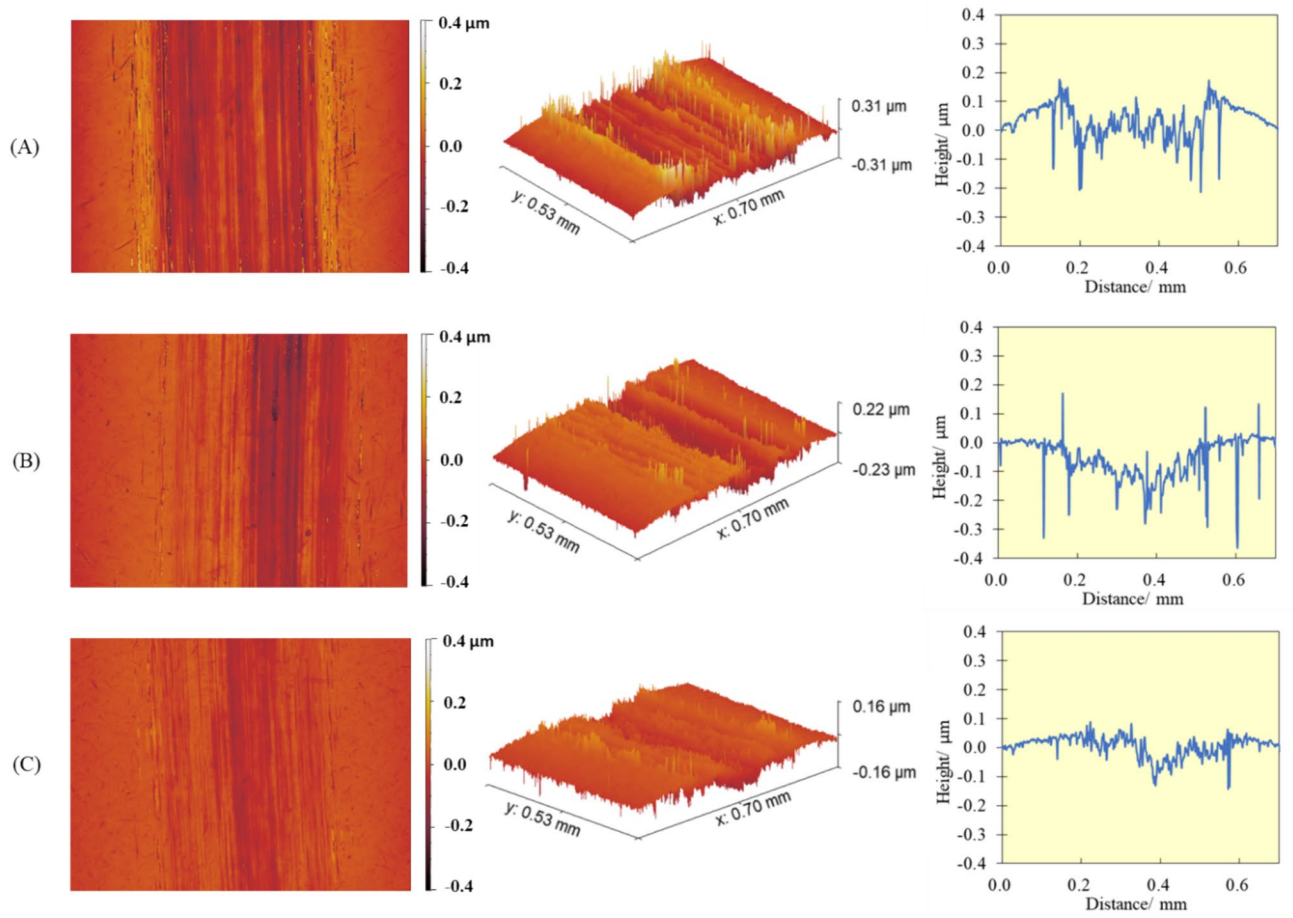

Fig. 5 Wear profiles of the steel balls (WLI images with 20× magnification) after long tribological tests (4 h) at an entrainment speed of 10 mm·s^{-1}, under the load of 50 N using as lubricants: **(A)** PEG200 + 1%RC 4801, **(B)** PEG 200 + 2%[C_6-4-pic][TfO] + 1%RC 4801, and **(C)** PEG 200 + 2% [C_6mim][TfO] + 1%RC 4801. *Z* scale is 1000× magnified compared to lateral scale

In Fig. 5, the WLI images and wear profiles of the balls and disks are shown, respectively. The mixtures containing ILs led to narrower and less deep wear profiles on both ball and disk comparing to neat PEG 200 + 1%RC 4801, especially the one containing [C_6mim][TfO]. In all cases, the images suggest the existence of both abrasive and adhesive wear. Analyzing Fig. 6, it is possible to observe that the abrasive component decreases from PEG 200 to [C_6mim][TfO], with less deep wear grooves, indicating an increased surface protection.

The wear tracks on the disks were also analyzed by optical microscopy to check for indications of tribofilm formation or other changes to the interface (see Fig. 7). The mechanisms of tribofilm formation by ionic liquids on steel surfaces have been discussed by several authors [26–29]. According to those authors, high oxygen content in tribofilms was observed and attributed to substantial oxidation during the tribological tests. The tribofilms were assumed to form through the reaction of oxygen from phosphate groups in the ILs with the iron surface and/or iron wear debris, suggested by the metallic Fe peaks observed in XPS. However, other authors recently reported that no chemical reaction occurred between phosphonium-based ILs and the steel surface during nanotribological experiments carried out by Li et al. [30], who conducted nanoscale single asperity studies using atomic force microscopy (AFM) of sliding in a pure IL, [$P_{6,6,6,14}$][DEHP], on steel. Taking advantage of the in situ capability of the AFM, they verified that friction reduction only occurred after the tip removes the steel's native oxide layer. After that, chemical imaging produced no evidence for the stress-assisted, thermally activated chemical formation of a tribofilm. Instead, the removal of the native oxide layer of the steel led to an increase in surface roughness, adsorption of the IL on the metallic Fe, and formation of a densely packed adsorbed IL layer that reduced friction and wear.

In our tests, no evidence of tribofilm formation is detected for PEG 200 + 1%RC 4801. However, a bluish color can be observed on the wear tracks for the tests carried out with both ILs added to PEG 200 + 1%RC 4801. This may suggest

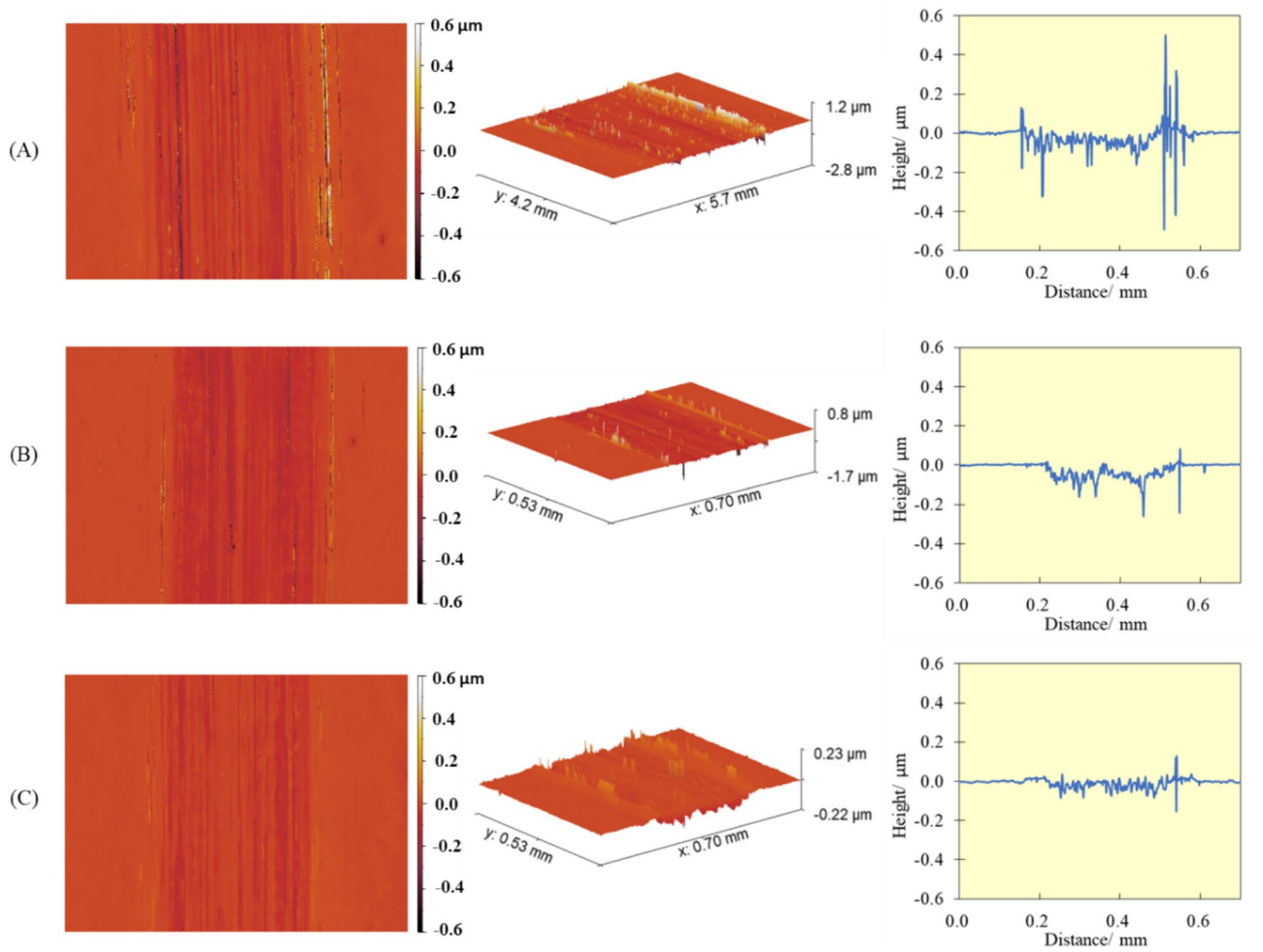

Fig. 6 Wear profiles of the steel disks (WLI images with 20× magnification) after long tribological tests (4 h) at an entrainment speed of 10 mm·s^{-1}, under the load of 50 N using as lubricants: **(A)** PEG200 + 1%RC 4801, **(B)** PEG 200 + 2% [C_6-4-pic][TfO] + 1%RC 4801, and **(C)** PEG 200 + 2% [C_6mim][TfO] + 1%RC 4801. *Z* scale is 1000 × magnified compared to lateral scale

the presence of a tribofilm, as reported by other authors who investigated the formation of zinc dialkyldithiophosphate (ZDDP) tribofilms [31–33] or could be due to an adsorbed film comprised of ILs, as suggested in [30]. It is also possible that the bluish color might be due to the different thickness and optical properties of the surface oxide layer which may have been modified by the sliding process.

In order to investigate this, XPS analysis of the neat ILs, as well as the inside of the wear tracks, was performed. The spectra were compared for N 1 s and S 2p species (see Figure S4). The N 1 s is a single peak at *ca*. 402 eV for the neat ILs, but for the wear tracks, the main peak is shifted to 400 eV. This can be due to tribochemical reactions between the ILs and Fe from the steel surface, leading to the formation of Fe–N bonds, as reported by other authors [34]. However, we cannot exclude the possibility of the shift deriving from the presence of adsorbed contaminants and degradation products of the ILs. Regarding the width of the peak, the binding energy range includes the value representative of the ILs, but its width suggests the presence of more species, such as nitrogen-containing organic compounds [35]. Regarding S 2p, there is no detectible S for [C_6-4-pic][TfO], but the inside of the wear track for [C_6mim][TfO] shows a peak at *ca*. 169 eV, which is in agreement with the presence of $FeSO_4$ and $Fe_2(SO_4)_3$ species [36], probably derived from tribochemical reactions, which suggests the formation of a tribofilm.

The relative atomic percentages of the primary elements found inside the wear tracks are presented in Table 1. Fe, C, and O are originally present on the bearing steel disks. Inside the wear tracks on the disks lubricated with both IL additives, both N and S signals are detected, suggesting that the two cations and the anion take an active part on the film formation, as proposed by other authors [26].

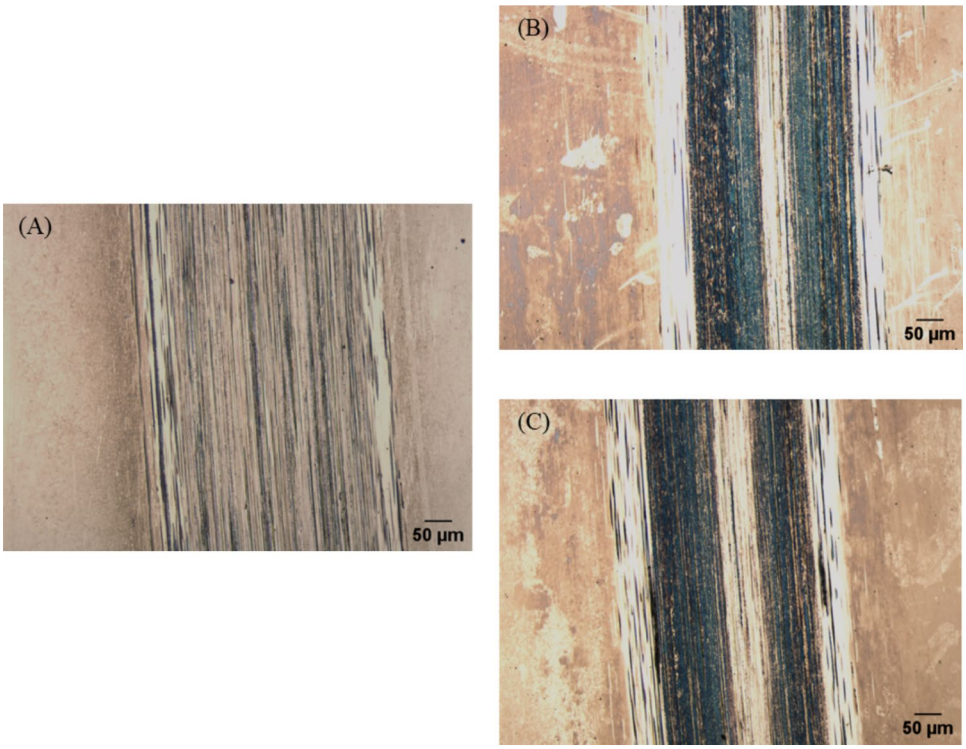

Fig. 7 Optical microscopy images (10× magnification) of the wear tracks after the tribological tests for **(A)** PEG 200 + 1%RC 4801, **(B)** PEG 200 + 2% [C_6-4-pic][TfO] + 1%RC 4801, and **(C)** PEG 200 + 2% [C_6mim][TfO] + 1%RC 4801

Table 1 Relative surface atomic concentrations inside the wear tracks

Lubricant	Relative atomic percentages				
	Fe 2p	O 1s	C 1s	N 1s	S 2p
PEG200 + 1% RC 4801	7.78	33.32	58.90	-	-
PEG200 + 2% [C_6-4-pic][TfO] + 1%RC 4801	1.63	27.64	70.39	0.25	0.09
PEG200 + 2% [C_6mim][TfO] + 1%RC 4801	3.41	29.87	65.60	0.97	0.14

Although small, the atomic percentages from the N 1 s and S 2p peaks are higher for the better performing mixture, PEG 200 + 2% [C_6mim][TfO] + 1% RC 4801, indicating that this IL has a greater tendency to adsorb to the steel surface, as previously reported by other authors [37].

The higher strength of the N 1 s peak compared to that of S 2p suggests that the IL interacts preferentially with the steel surface through the N-containing cation, although the S-containing anion participates in the adsorption as well. The formation of the adsorbed film helps in the protection of the steel surfaces, leading to a decrease in friction and wear.

Regarding Fe 2p signals, no definite evidence of Fe–N and Fe–S bonds exists, making tribofilm formation less likely. The appearance of nitrogen and sulfur emissions, in particular for the sample using [C_6mim][TfO] are in agreement with the presence of an IL adsorbed layer, which partially covers the underlying iron oxide. To more deeply understand the chemical species formed, deconvolution of Fe, C, and O peaks, inside and outside the wear tracks, was performed and is shown in Fig. 8 and Figure S5, respectively, for [C_6mim][TfO] and for PEG 200 and [C_6-4-pic][TfO].

The deconvolution of Fe 2p used the guidelines and peak shapes of Biesinger et al., considering metallic Fe, FeO, Fe_2O_3, and FeOOH as possible chemical states [38]. Since Fe_2O_3 and FeOOH both have Fe^{3+}, their respective atomic percentages are summed up to represent the total amount of Fe^{3+} (Table S1, Supporting Information). Comparing the outside of the wear tracks for each of the disks from the three experiments, different amounts of iron oxidation states are found. This is attributed to local variations of the corrosion on the iron surfaces. For this reason, absolute values are not considered, but rather, changes that occur to the mix of oxidation states due to wear (i.e., the values given are the % change inside each wear track relative to outside for each sample). These changes are presented in Table 2.

The iron oxidation states remain practically the same after wear in case of PEG200 + 1% RC 4801 (within 2%). Using PEG200 + 2% [C_6-4-pic][TfO] + 1%RC 4801, a noticeable partial reduction of Fe^{3+} to Fe^{2+} can be observed, without

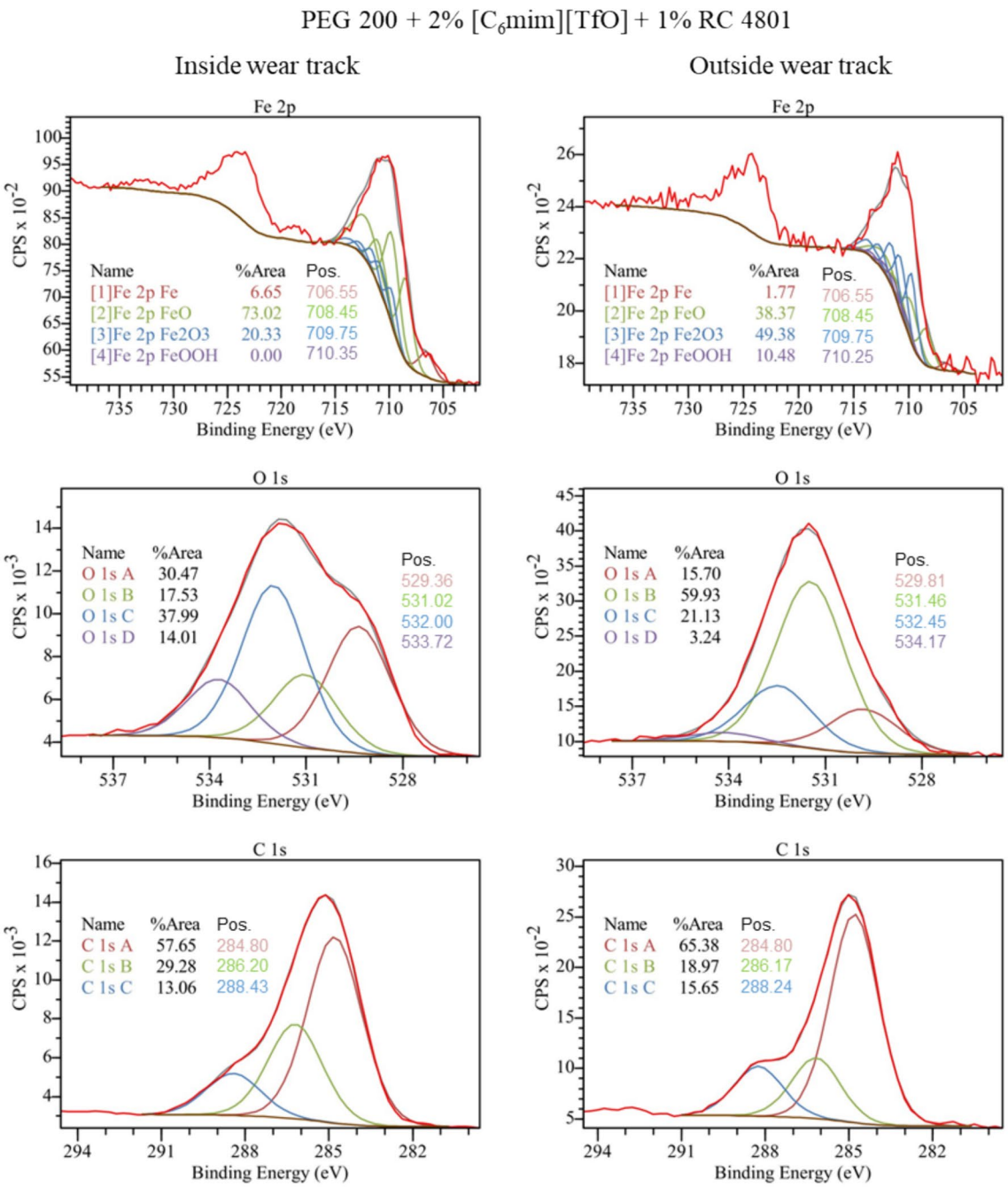

Fig. 8 XPS spectra for inside (left spectra) and outside (right spectra) the wear tracks for PEG 200 + 2% [C_6mim][TfO] + 1%RC4801

the formation of metallic Fe. With PEG200 + 2% [C_6mim][TfO] + 1%RC 4801, even more Fe^{3+} is reduced to Fe^{2+} and metallic Fe is also formed.

Correlating these observations with the performance of the lubricants, it appears that better lubrication is achieved in cases where stronger reduction of the disk surface occurs. A potential explanation may lie within the mechanical properties of the involved materials: FeO has lower hardness and is more ductile than Fe_2O_3 and thus increases surface protection against friction and wear.[39] The presence of [C_6mim][TfO] in the lubricant mixture, which causes the highest iron oxide (and hydroxide) reduction, increases the amount of Fe_2O_3 on the surface, leading to the best tribological behavior.

Outside the wear track, IL [C_6mim][TfO] establishes hydrogen bonding interactions with the steel surface, since the methylimidazolium cation has an acidic proton (located in the H2 of the imidazole ring). In addition to that, inside

Table 2 Changes to Fe^0, Fe^{2+}, and Fe^{3+} oxidation states inside the wear tracks for the three mixtures

Lubricant	Changes to iron oxidation states (%)		
	Fe^0	Fe^{2+}	Fe^{3+}
PEG200 + 1% RC 4801	+0.29	−2.02	+1.71
PEG200 + 2% [C_6-4-pic][TfO] + 1%RC 4801	+0.25	+19.87	−20.13
PEG200 + 2% [C_6mim][TfO] + 1%RC 4801	+4.88	+24.17	−29.05

the wear track, a reduction of iron is observed (from Fe^{3+} to Fe^{2+}) because of the presence of this IL in the system. The reduction of metals in the presence of imidazolium and pyridinium-based ILs has been previously reported in the literature [40] and may be responsible for the improved tribological performance.

It is important to stress that the lubrication capacity of ILs may derive from two processes: (i) chemical alteration of the surface leading to tribofilm formation, (ii) adsorption of the IL to form an interfacial lubricious layer. The optical microscopy images suggest the formation of a tribofilm, but we cannot rule out the possibility of the existence of an ordered absorbed layer combined with oxidation of the substrate. Indeed, the possibility of establishing H bonds between [C_6mim][TfO] and the steel surface, due to the existence of an acidic proton, indicates the stronger ability of this IL to adsorb to the surface. Thus, the formation of a lubricating film by the ILs is evident, but we are not able to identify unambiguously the nature of this film. Furthermore, we must stress that at high pressures and temperatures the lubrication mechanisms are complex and further studies are needed to understand the friction and wear mechanisms.

3 Conclusion

The tribological performance of two ILs was studied for 52,100 steel contacts. It is well known that ILs are corrosive of steel, so a succinic acid derivative corrosion inhibitor was added to prevent corrosion. Two ILs—[C_6mim][TfO] and [C_6-4-pic][TfO]—were tested with 1 wt.% corrosion inhibitor as anti-wear additives in base oil PEG 200 and revealed interesting lubricating properties. PEG 200 + 2% [C_6mim][TfO] + 1% RC4801 reduced friction by 12% and more substantially, reduced wear up to ~ 76%, thus acting as an anti-wear additive. On the other hand, PEG 200 + 2% [C_6-4-pic][TfO] + 1% RC4801 led to slightly increased friction, but still reduced wear up to ~ 46% when comparing to neat PEG 200 + 1% RC4801 and thus also acted as an anti-wear additive. XPS analysis allowed to conclude that [C_6mim][TfO] has a higher tendency to form an adsorbed film, which may be what reduced the amount of wear for the underlying steel surface.

The results obtained with the two ILs open opportunities to explore these environmentally friendly compounds as potential lubricants for steel tribological components. These ILs were able to reduce wear of the steel surfaces under extreme pressure conditions (1.12 GPa) as long as some antioxidant was added. This is of substantial importance for several industries due to lowering the costs in replacing steel parts.

4 Experimental Section

4.1 Materials

All reagents for the synthesis of ILs were purchased and used without additional purification. The list of reagents is as the following: 4-methylpyridine 98% from Alfa Aesar (Tewksbury, MA, USA), methylimidazole 99% from Alfa Aesar (Tewksbury, MA, USA), and sulfuric acid 95–97% from Merck (Rahway, NJ, USA).

The solvents were acetonitrile 99.8% from Merck (Darmstadt, Germany) and deuterated water 99.9% from Eurisotop (Gif sur Yvette, France). Polyethylene glycol (MW 200)—PEG200 was from Sigma-Aldrich (Rahway, NJ, USA), with water content < 0.5%. Corrosion inhibitor Additin® RC 4801 was from Lanxess (Pittsburgh, PA, USA). Distilled and deionized water (DD) was obtained with a Millipore system.

4.2 Synthesis

The syntheses of ILs [C_6mim][TfO], [C_6-4-pic][TfO], and [4-picH][HSO_4] were described in previous works [7, 20].

4.3 Methods

Corrosion tests were performed by deposition of two or three droplets of the ILs, with and without corrosion inhibitor RC 4801, on steel disks for 48 h. Afterward, the steel samples were carefully washed with toluene and isopropanol, each for 10 min, in an ultrasound bath.

The viscosity of the liquids (PEG + corrosion inhibitor and ILs as 2 wt% in PEG + corrosion inhibitor) was measured using a rheometer MCR 92 (Anton Paar, Graz, Austria). The results are average values obtained from three measurements.

The water content of the ILs as 2 wt% in PEG was checked by Karl–Fischer coulometric titration (Metrohom,

Switzerland). All the studied solutions were saturated in terms of water content, around 2 wt%.

The tribological tests were conducted in an MTM (PCS Instruments, London, UK) that was used to measure traction coefficients under specified conditions. The MTM is a ball-on-disk tribometer presented in Figure S6 (Supporting Information), in which the rotation of the ball is independent to the rotation of the disk, enabling access to a range of slide-to-roll ratios (SRR). Space Layer Imaging (SLIM) was carried out during the tribological tests, but the films were so thin that SLIM could not detect the thickness. 52,100 steel highly polished balls (19.05 mm diameter, RMS = 0.5 ± 0.2 nm) and disks (46 mm diameter, RMS = 0.5 ± 0.2 nm) from PCS Instruments (London, UK) were used for the tribological tests. The balls and disks were AISI/ASTM 52100 bearing steel which is a high carbon and manganese (C, Mn 0.95–1.1%) steel alloy, containing low levels of silicon and chromium (Si, Cr ≤ 0.35%).

Stribeck curve measurements were performed at 60 °C, over a wide range of speeds (from 2000 to 7 $mm{\cdot}s^{-1}$ entrainment speed), SRR of 50% and an applied load of 50 N, yielding a Hertzian maximum contact pressure of 1.12 GPa. All other MTM measurements were carried out at an entrainment speed of 10 $mm{\cdot}s^{-1}$. Prior to testing, the specimen (balls and disks) and the removable MTM components were cleaned by sonication for 10 min in each of toluene and 2-propanol. All parts were wiped with a Kimwipe after the cleaning process, and residual fibers were removed by blowing with compressed nitrogen gas. The MTM pot was rinsed in toluene followed by 2-propanol and dried by blowing with compressed nitrogen gas. This rinsing and drying procedure was performed three times or until the lubricants were removed completely.

After the tribological tests, the tracks were imaged with white light interferometry using a Zygo NewView 6300 Interferometer with a 20 × objective and 0.5 × internal multiplier, yielding a magnification level of 10 × and a 530 µm × 700 µm field of view. The images were analyzed using software program Gwyddion [41]. The MTM balls were imaged with a vertical scan range of 150 µm and the images were leveled through a spherical subtraction in Gwyddion.

A BX51 Optical Microscope (Olympus, Florida, USA) was used to assess the tribofilm formation on the wear tracks after the tribological tests. The images were analyzed using ImageJ software [42].

The elemental composition of the wear tracks on the 52,100 steel disks was studied by X-ray photoelectron spectroscopy (XPS), using an Axis Supra spectrometer (Kratos Analytical Ltd., Manchester, UK). A monochromatic Al Kα source was run at 150 W. The detailed spectra were acquired at a pass energy of 160 eV through an aperture of 110 µm. Data analysis was done with CasaXPS. Atomic percentages were calculated assuming a homogenous distribution of elements, using the Kratos relative sensitivity factors. Due to the appearance of differential charging in some for the samples, all binding energies were corrected to C 1 s at 284.8 eV.

Supplementary Information The online version contains supplementary material available at https://doi.org/10.1007/s11249-024-01898-6.

Acknowledgements The work was supported by the Portuguese Foundation for Science and Technology (FCT) through the projects UIDB/00100/2020, UIDP/00100/2020, and IMS-LA/P/0056/2020 and through the PhD grant SFRH/BD/140079/2018 for Mariana Donato. Additionally, this work was supported by national funds from FCT in the scope of the projects UIDB/50022/2020 (IDMEC/LAETA) and LA/P/0037/2020, UIDP/50025/2020, and UIDB/50025/2020 of the Associate Laboratory Institute of Nanostructures, Nanomodelling and Nanofabrication – i3N. In addition, RWC and PN acknowledge support from the US Department of Energy under grant number DE-EE0010211.

Author Contributions M. T. D.—Investigation, Methodology, Validation, Visualization, and Writing – original draft; P. N.—Investigation, Methodology, and Validation; J. D.—Investigation, Methodology, and Validation; L. C. B.—Supervision, Conceptualization, Methodology, and Writing – review & editing; B. S.—Supervision, Conceptualization, Methodology, and Writing – review & editing; R. C.—Supervision, Conceptualization, Methodology, and Writing – review & editing; R. W. C.—Supervision, Conceptualization, Methodology, and Writing – review & editing.

Funding The work was supported by the Portuguese Foundation for Science and Technology (FCT) through the projects UIDB/00100/2020, UIDP/00100/2020, and IMS-LA/P/0056/2020 and through the PhD grant SFRH/BD/140079/2018 for Mariana Donato. Additionally, this work was supported by the national funds from FCT in the scope of the projects UIDB/50022/2020 (IDMEC/LAETA) and LA/P/0037/2020, UIDP/50025/2020, and UIDB/50025/2020 of the Associate Laboratory Institute of Nanostructures, Nanomodelling and Nanofabrication – i3N. In addition, RWC and PN acknowledge support from the US Department of Energy under grant number DE-EE0010211.

Data Availability No datasets were generated or analyzed during the current study.

Declarations

Competing interest The authors declare no competing interests.

References

1. Panda, A., Sahoo, A.K., Kumar, R., Das, R.K.: A review on machinability aspects for AISI 52100 bearing steel. Mater. Today Proc. **23**, 617–621 (2020). https://doi.org/10.1016/j.matpr.2019.05.422
2. Ferreira, R., Carvalho, Ó., Pires, J., Sobral, L., Carvalho, S., Silva, F.: A new tribometer for the automotive industry: development and experimental validation. Exp. Mech. **62**, 483–492 (2022). https://doi.org/10.1007/s11340-021-00805-7
3. Tung, S.C., McMillan, M.L.: Automotive tribology overview of current advances and challenges for the future. Tribol. Int. **37**, 517–536 (2004). https://doi.org/10.1016/j.triboint.2004.01.013
4. Zhou, Y., Qu, J.: Ionic liquids as lubricant additives: a review. ACS Appl. Mater. Interfaces **9**, 3209–3222 (2017). https://doi.org/10.1021/acsami.6b12489
5. Wijanarko, W., Khanmohammadi, H., Espallargas, N.: Ionic liquid additives in water-based lubricants for bearing steel—effect of electrical conductivity and ph on surface chemistry friction and wear. Front. Mech. Eng. **7**, 756929 (2022). https://doi.org/10.3389/fmech.2021.756929
6. Antunes, M., Donato, M.T., Paz, V., Caetano, F., Santos, L., Colaço, R., Branco, L.C., Saramago, B.: Improving the lubrication of silicon surfaces using ionic liquids as oil additives: the effect of sulfur-based functional groups. Tribol. Lett. **68**, 70 (2020). https://doi.org/10.1007/s11249-020-01308-7
7. Donato, M.T., Caetano, F., Colaço, R., Branco, L.C., Saramago, B.: Picolinium-based hydrophobic ionic liquids as additives to PEG200 to lubricate steel-silicon contacts. ChemistrySelect **5**, 5864–5872 (2020). https://doi.org/10.1002/slct.202000613
8. Donato, M.T., Santos, L., Diogo, H.P., Colaço, R., Branco, L.C., Saramago, B.: Eutectic systems containing an ionic liquid and PEG200 as lubricants for silicon surfaces: effect of the mixture's molar ratio. J. Mol. Liq. **350**, 118572 (2022). https://doi.org/10.1016/j.molliq.2022.118572
9. Donato, M.T., Colaço, R., Branco, L.C., Saramago, B.: A review on alternative lubricants: Ionic liquids as additives and deep eutectic solvents. J. Mol. Liq. **333**, 116004 (2021). https://doi.org/10.1016/j.molliq.2021.116004
10. Lawes, S.D.A., Hainsworth, S.V., Blake, P., Ryder, K.S., Abbott, A.P.: Lubrication of steel/steel contacts by choline chloride ionic liquids. Tribol. Lett. **37**, 103–110 (2010). https://doi.org/10.1007/s11249-009-9495-6
11. Sierra, A., Coleman, M.G., Iglesias, P.: Tribological properties of borate-based protic ionic liquids as neat lubricants and biolubricant additives for steel-steel contact. Lubricants **10**, 269 (2022). https://doi.org/10.3390/lubricants10100269
12. Yao, M., Liang, Y., Xia, Y., Zhou, F.: Bisimidazolium ionic liquids as the high-performance Antiwear additives in poly(ethylene glycol) for steel−steel contacts. ACS Appl. Mater. Interfaces **1**, 467–471 (2009). https://doi.org/10.1021/am800132z
13. Weng, L., Liu, X., Liang, Y., Xue, Q.: Effect of tetraalkylphosphonium based ionic liquids as lubricants on the tribological performance of a steel-on-steel system. Tribol. Lett. **26**, 11–17 (2007). https://doi.org/10.1007/s11249-006-9175-8
14. Khan, A., Gusain, R., Sahai, M., Khatri, O.P.: Fatty acids-derived protic ionic liquids as lubricant additive to synthetic lube base oil for enhancement of tribological properties. J. Mol. Liq. **293**, 111444 (2019). https://doi.org/10.1016/j.molliq.2019.111444
15. Kreivaitis, R., Gumbytė, M., Kupčinskas, A., Kazancev, K., Ta, T.N., Horng, J.H.: Investigation of tribological properties of two protic ionic liquids as additives in water for steel–steel and alumina–steel contacts. Wear **456–457**, 203390 (2020). https://doi.org/10.1016/j.wear.2020.203390
16. Guo, H., Pang, J., Adukure, A.R., Iglesias, P.: Influence of hydrogen bonding and ionicity of protic ionic liquids on lubricating steel-steel and steel-aluminum contacts: potential ecofriendly lubricants and additives. Tribol. Lett. **68**, 114 (2020). https://doi.org/10.1007/s11249-020-01354-1
17. Guo, H., Iglesias, P.: Tribological behavior of ammonium-based protic ionic liquid as lubricant additive. Friction. **9**, 169–178 (2021). https://doi.org/10.1007/s40544-020-0378-z
18. Fang, H., Li, Y., Zhang, S., Ding, Q., Hu, L.: Lubricating performances of oil-miscible trialkylanmmonium carboxylate ionic liquids as additives in PAO at room and low temperatures. Appl. Surf. Sci. **568**, 150922 (2021). https://doi.org/10.1016/j.apsusc.2021.150922
19. Li, Z., Mangolini, F.: Recent advances in nanotribology of ionic liquids. Exp. Mech. **61**, 1093–1107 (2021). https://doi.org/10.1007/s11340-021-00732-7
20. Donato, M.T., Deuermeier, J., Colaço, R., Branco, L.C., Saramago, B.: New protic ionic liquids as potential additives to lubricate SI-based MEMS/NEMS. Molecules **28**, 2678 (2023). https://doi.org/10.3390/molecules28062678
21. Zaretsky, E.V.: Rolling bearing steels: a technical and historical perspective. Mater. Sci. Technol. **28**, 58–69 (2012). https://doi.org/10.1179/1743284711Y.0000000043
22. Uerdingen, M., Treber, C., Balser, M., Schmitt, G., Werner, C.: Corrosion behaviour of ionic liquids. Green Chem. **7**, 321 (2005). https://doi.org/10.1039/b419320m
23. Arenas, M.F., Reddy, R.G.: Corrosion of steel in ionic liquids. J. Min. Metall. Sect. B **39**, 81–91 (2003). https://doi.org/10.2298/JMMB0302081A
24. Hamrock, B.J., Dowson, D.: Isothermal elastohydrodynamic lubrication of point contacts: part III—fully flooded results. J. Lubr. Technol. **99**, 264–275 (1977). https://doi.org/10.1115/1.3453074
25. Spikes, H.A., Spikes, G.G.: The control of friction by molecular fractionation of base fluid mixtures at metal surfaces. Tribol. Trans. **40**, 461–469 (2008). https://doi.org/10.1080/10402009708983681
26. Zhou, Y., Dyck, J., Graham, T.W., Luo, H., Leonard, D.N., Qu, J.: Ionic liquids composed of phosphonium cations and organophosphate, carboxylate, and sulfonate anions as lubricant antiwear additives. Langmuir **30**, 13301–13311 (2014). https://doi.org/10.1021/la5032366
27. Barnhill, W.C., Qu, J., Luo, H., Meyer, H.M., Ma, C., Chi, M., Papke, B.L.: Phosphonium-organophosphate ionic liquids as lubricant additives: effects of cation structure on physicochemical and tribological characteristics. ACS Appl. Mater. Interfaces **6**, 22585–22593 (2014). https://doi.org/10.1021/am506702u
28. Qu, J., Barnhill, W.C., Luo, H., Meyer, H.M., Leonard, D.N., Landauer, A.K., Kheireddin, B., Gao, H., Papke, B.L., Dai, S.: Synergistic effects between phosphonium-alkylphosphate ionic liquids and zinc dialkyldithiophosphate (ZDDP) as lubricant additives. Adv. Mater. **27**, 4767–4774 (2015). https://doi.org/10.1002/adma.201502037
29. Guo, W., Zhou, Y., Sang, X., Leonard, D.N., Qu, J., Poplawsky, J.D.: Atom probe tomography unveils formation mechanisms of wear-protective tribofilms by ZDDP, ionic liquid, and their combination. ACS Appl. Mater. Interfaces **9**, 23152–23163 (2017). https://doi.org/10.1021/acsami.7b04719
30. Li, Z., Dolocan, A., Morales-Collazo, O., Sadowski, J.T., Celio, H., Chrostowski, R., Brennecke, J.F., Mangolini, F.: Lubrication mechanism of phosphonium phosphate ionic liquid in nanoscale single-asperity sliding contacts. Adv. Mater. Interfaces **7**, 2000426 (2020). https://doi.org/10.1002/admi.202000426
31. Hsu, C.-J., Stratmann, A., Rosenkranz, A., Gachot, C.: Enhanced growth of ZDDP-based tribofilms on laser-interference patterned cylinder roller bearings. Lubricants. **5**, 39 (2017). https://doi.org/10.3390/lubricants5040039

32. Lorenz, M., Pawlicki, A.A., Hysmith, H.E., Cogen, K., Thaker, H., Ovchinnikova, O.S.: Direct multimodal nanoscale visualization of early phosphorus-based antiwear tribofilm formation. ACS Appl. Mater. Interfaces **14**, 35157–35166 (2022). https://doi.org/10.1021/acsami.1c16761
33. Kubiak, K.J., Mathia, T.G., Bigerelle, M.: Influence of roughness on ZDDP tribofilm formation in boundary lubricated fretting. Tribol. Mater. Surf. Interfaces **6**, 182–188 (2012). https://doi.org/10.1179/1751584X12Y.0000000020
34. Artyushkova, K., Kiefer, B., Halevi, B., Knop-Gericke, A., Schlogl, R., Atanassov, P.: Density functional theory calculations of XPS binding energy shift for nitrogen-containing graphene-like structures. Chem. Commun. **49**, 2539 (2013). https://doi.org/10.1039/c3cc40324f
35. Arcifa, A., Rossi, A., Espinosa-Marzal, R.M., Spencer, N.D.: Influence of environmental humidity on the wear and friction of a silica/silicon tribopair lubricated with a hydrophilic ionic liquid. ACS Appl. Mater. Interfaces **8**, 2961–2973 (2016). https://doi.org/10.1021/acsami.5b09370
36. Naumkin, A.V., Kraut-Vass, A., Gaarenstroom, S.W., Powell, C.J.: NIST standard reference database 20, version 4.1, https://srdata.nist.gov/xps/ElmComposition
37. Mashuga, M., Olasunkanmi, L., Adekunle, A., Yesudass, S., Kabanda, M., Ebenso, E.: Adsorption, thermodynamic and quantum chemical studies of 1-hexyl-3-methylimidazolium based ionic liquids as corrosion inhibitors for mild steel in HCl. Materials. **8**, 3607–3632 (2015). https://doi.org/10.3390/ma8063607
38. Biesinger, M.C., Payne, B.P., Grosvenor, A.P., Lau, L.W.M., Gerson, A.R., Smart, R.S.T.C.: Resolving surface chemical states in XPS analysis of first row transition metals, oxides and hydroxides: Cr, Mn, Fe Co and Ni. Appl. Surf. Sci. **257**, 2717–2730 (2011). https://doi.org/10.1016/j.apsusc.2010.10.051
39. Vergne, C., Boher, C., Gras, R., Levaillant, C.: Influence of oxides on friction in hot rolling: experimental investigations and tribological modelling. Wear **260**, 957–975 (2006). https://doi.org/10.1016/j.wear.2005.06.005
40. Vicente, J.D.S., Miguel, D.C., Gonçalves, A.M.P., Cabrita, D.M., Carretas, J.M., Vieira, B.J.C., Waerenborgh, J.C., Belo, D., Gonçalves, A.P., Leal, J.P.: On the dissolution of metals in ionic liquids 1: iron, cobalt, nickel, copper, and zinc. Sustain. Chem. **2**, 63–73 (2021). https://doi.org/10.3390/suschem2010005
41. Nečas, D., Klapetek, P.: Gwyddion: an open-source software for SPM data analysis. Open Phys. (2012). https://doi.org/10.2478/s11534-011-0096-2
42. Schneider, C.A., Rasband, W.S., Eliceiri, K.W.: NIH Image to ImageJ: 25 years of image analysis. Nat. Methods **9**, 671–675 (2012). https://doi.org/10.1038/nmeth.2089

Authors and Affiliations

Mariana T. Donato[1,2,3] · Pranjal Nautiyal[3] · Jonas Deuermeier[4] · Luís C. Branco[2] · Benilde Saramago[1] · Rogério Colaço[5] · Robert W. Carpick[3]

✉ Rogério Colaço
rogerio.colaco@tecnico.ulisboa.pt

✉ Robert W. Carpick
carpick@seas.upenn.edu

[1] Departamento de Engenharia Química, Instituto Superior Técnico, Institute of Molecular Sciences, Centro de Química Estrutural, Universidade de Lisboa, Av. Rovisco Pais, 1049-001 Lisbon, Portugal

[2] Departamento de Química, LAQV-REQUIMTE, NOVA School of Science and Technology, Universidade NOVA de Lisboa, Campus da Caparica, 2829-516 Caparica, Portugal

[3] Department of Mechanical Engineering & Applied Mechanics, University of Pennsylvania, Philadelphia, PA 19104, USA

[4] Departamento de Ciência Dos Materiais, CENIMAT\i3N and CEMOP/UNINOVA, NOVA School of Science and Technology, Universidade NOVA de Lisboa, Campus da Caparica, 2829-516 Caparica, Portugal

[5] Departamento de Engenharia Mecânica, Instituto Superior Técnico, IDMEC-Instituto de Engenharia Mecânica, Universidade de Lisboa, Av. Rovisco Pais, 1049-001 Lisbon, Portugal